ЖУРНАЛ СТРУКТУРНОЙ ХИМИИ

2014. Том 55, № 4 *Июль – август* *С. 656 – 663*

UDC 541.6:547.13:546.57

PROPERTIES OF THE SILVER CYCLIC AMIDE $Ag_2(C_4H_4NO_2)_2(H_2O)$ CRYSTAL FROM THE PERIODIC DFT COMPUTATIONS

A. Stashans[1], D. Castillo[1,2]

[1]*Grupo de Fisicoquímica de Materiales, Universidad Técnica Particular de Loja, Apartado 11-01-608, Loja, Ecuador*
E-mail: arvids@utpl.edu.ec
[2]*Escuela de Electrónica y Telecomunicaciones, Universidad Técnica Particular de Loja, Apartado 11-01-608, Loja, Ecuador*

Received March, 4, 2013 *Revised — April, 6, 2013*

A molecular crystal of silver cyclic amide $Ag_2(C_4H_4NO_2)_2(H_2O)$ is studied using first-principles density functional theory calculations within the generalized gradient approximation (GGA). A number of different exchange-correlation functionals are considered for a possible treatment of the system. It is found that the Perdew—Burke—Ernzerhof (PBE) GGA exchange-correlation functionals are adequate for the $Ag_2(C_4H_4NO_2)_2(H_2O)$ crystal. The results obtained show the possibility to reproduce rather well the geometry of at least some molecular crystals by means of the periodic solid-state calculations if the computational parameters are chosen adequately. The present work also reports the analysis of the chemical bonding in the material and gives the total and partial density of states. Our solid-state computations point out the possible magnetic properties of the molecular crystal under study.

K e y w o r d s: crystal structure, chemical bonding, electronic properties, magnetism, DFT.

INTRODUCTION

Organometallic compounds have recently found numerous applications in different areas. Silver(I)—N and silver(I)—O bonding materials are the known potential bioinorganic materials [1, 2] that are mostly light-sensitive, especially in solution, and their characterization is not easily performed. Silver(I) ions have long been known to have inhibitory and bacterial effects [1, 3], while silver (I) compounds also show antimicrobial activities [4—6].

Despite a progress in the experimental synthesis and molecular design of different silver(I) molecular crystals [6—15] a better understanding of these systems is needed at the fundamental quantum scale. The quantum mechanical treatment of condensed-phase systems nowadays is largely restricted to the quantum mechanical method known as the density functional theory (DFT). It has become the method of choice for electronic structure calculations across an unusually wide variety of fields, from organic chemistry [16] to condensed matter physics [17]. There are two main reasons for the success of DFT [18]: first, DFT offers the only currently known practical method of fully quantum mechanical calculations for systems with many hundreds or even thousands of electrons. Second, it enhances our understanding by relying on relatively simple, physically accessible quantities that are easily visualized even for very large systems [19].

On the other hand, the prediction of molecular crystal structures computationally has been considered an impossible mission [20]. In particular, there exist some suggestions that DFT cannot deal accurately with systems such as molecular crystals due to inadequate treatment of the van der Waals forces, which are weak intermolecular forces arising from quantum-induced instantaneous polarization

multipoles in molecules and are rather important in molecular and organic systems in the ambient state [21]. The error might lead to incorrect geometric and lattice parameters for a given system. As a result, molecular structure computations mainly based on the GAUSSIAN and GAMESS computer codes have been used up to now in order to study molecular crystals. Such computations, however, cannot predict the features arising due to the periodic nature of these compounds, e.g. electrical conductivity, magnetism and electronic band structure properties.

In the present work, we apply the periodic DFT technique to study the silver cyclic amide $Ag_2(C_4H_4NO_2)_2(H_2O)$ crystal [22] and to show that this approach is adequate for molecular crystals if the corresponding computational parameters such as cut-off energy, k-point grid as well as pseudopotentials are carefully chosen and optimised for a given system. To demonstrate the fact that the DFT method can describe reasonably well at least some molecular crystals is our main aim. If periodic DFT computations are able to reproduce sufficiently well the geometry of a given molecular crystal, then it allows the performance of very precise studies on electrical, electronic, magnetic, etc. features which could be of interest for the future scientific and technological inquiries.

OUTLINE OF THE METHOD

The Vienna *ab initio* Simulation Package (VASP) [23, 24] based on the DFT approach has been utilized in the present work. Within the current framework, valence electronic states are expanded in a set of periodic plane waves, and the interaction between the core electrons and the valence electrons is implemented through the projector augmented wave (PAW) method [25]. We encountered ourselves with a number of problems to find the cut-off kinetic energy and the *k*-point set for the system under study. As a result, we had to explore a number of pseudopotentials to find the one which would allow us to obtain the necessary computational parameters for the $Ag_2(C_4H_4NO_2)_2(H_2O)$ molecular crystal. In particular, we attempted to exploit the PAW method combined with electron-electron exchange-correlation described by the GGA and the local density approximation instead of GGA combined with the PAW method. However, these approaches did not allow us to find a necessary convergence for the cut-off energy up to 1000 eV. The exploitation of ultra-soft pseudopotentials permitted us to obtain the cut-off energy in the region of 850 eV, but we failed to get the necessary *k*-point grid for our system. Finally, the PAW method together with the Perdew—Burke—Ernzerhof (PBE) [26] GGA exchange-correlation functionals permitted us to extract both cut-off energy and *k*-point set for the system under study. The advantage of GGA introduced by Perdew et al. [26] is that it retains the correct features of the local spin density and combines them with the most energetically important features of gradient-corrected non-locality. This permits an accurate description of the linear response of the uniform electron gas, the correct behaviour under uniform scaling, and a smoother potential. The above mentioned factors appear to be significant in using these electron-electron exchange-correlation functionals for the molecular systems. Summarising, we can state that the computed cut-off kinetic energy was found to be 900 eV, converging the total energy to < 1 meV. The Γ-centred Monkhorst-Pack (MP) grid with a 0.03 $Å^{-1}$ separation was applied, which corresponds to a *k*-point mesh of 5×5×2 for the exploited 100-atom supercell of the $Ag_2(C_4H_4NO_2)_2(H_2O)$ crystal possessing the monoclinic $P2_1/n$ crystalline lattice. The above mentioned parameters were obtained through the atomic relaxation until all the forces were < 0.01 eV/Å and the equilibrium state of the system was achieved.

In order to take into account strong electronic correlation of the Ag *d* electrons, we included an intra-site Coulomb repulsion *U*-term on the *d* projector of the Ag atom [27]. Thus, we arrived to the so-called GGA+*U* method. In this approach, the on-site Coulomb interaction energy is

$$E^{\mathrm{GGA+U}} = E^{\mathrm{GGA}} + \frac{(\bar{U} - \bar{J})}{2} \sum_{\sigma} \mathrm{Tr}[\mathbf{n}^{\sigma}(1 - \mathbf{n}^{\sigma})], \quad (1)$$

where $\mathbf{n}^{\sigma}$ is the density matrix of the *d* electrons, σ is a spin index, and $\bar{U}, \bar{J}$ are the spherically averaged matrix elements of the screened Coulomb and exchange interactions respectively. In the present approach only the difference $U = (\bar{U}, \bar{J})$ is meaningful. We made use of *U* being 3.5 eV. This value was found to be adequate for our system since allowed a better reproduction of the crystal geometry and the stabilization of the compound.

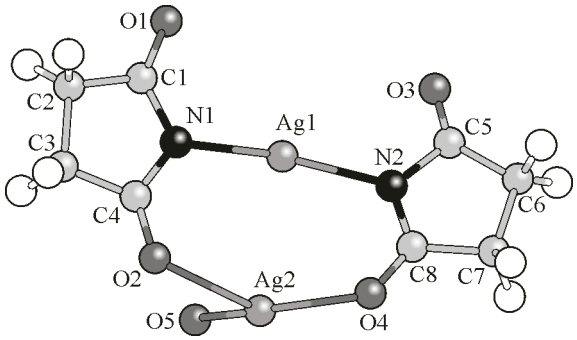

Fig. 1 (*left*). Schematic diagram of the butterfly-shaped $[Ag(C_4H_4NO_2)]_2$ dimer depicting the Ag atom vicinity

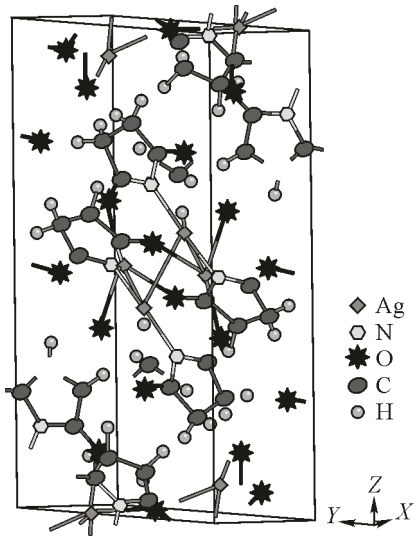

Fig. 2 (*right*). Primitive unit cell of the 100-atom $Ag_2(C_4H_4NO_2)_2(H_2O)$ crystal used throughout the study

RESULTS AND DISCUSSION

The structure of the $Ag_2(C_4H_4NO_2)_2(H_2O)$ crystal exhibits a butterfly-shaped $[Ag(C_4H_4NO_2)]_2$ dimer which contains an eight-membered ring (Fig. 1). One of the Ag atoms is four-coordinated having exclusively Ag—O bonds and the other is two-coordinated having exclusively Ag—N bonds. The multiple bonding capabilities of the groups in this ligand facilitates multiple ligand—Ag^+ contacts, including the intermolecular bonding via an Ag—O bond, yet water solubility is maintained. The supercell of 100 atoms used throughout the research coincides with the primitive unit cell (Fig. 2). We preferred to use high-precision (small spacing between k points in the reciprocal lattice, a large value of the cut-off energy, etc.) parameters instead of an extended supercell since the opposite choice would lead to a negative effect on the reliability of our results for the electronic and magnetic properties. Within our DFT+U computations we managed to reproduce quite well the equilibrium geometry of this molecular crystal. The monoclinic crystal lattice (space group $P2_1/n$) parameters were found to be $a = 8.74$ Å, $b = 8.09$ Å, and $c = 17.82$ Å, which are rather close to the experimentally predicted values of $a = 7.6776$ Å, $b = 8.0431$ Å, and $c = 17.8184$ Å [22]. The computationally obtained cell volume is found to be about 1258.94 Å^3, which is somewhat larger compared to the experimentally determined value of 1089.83 Å^3 [22]. The main bond length distances and principal angles formed by the chemical bonds are given in Tables 1 and 2 respectively. As one can observe, we managed to reproduce sa-

Table 1

Selected bond lengths obtained by the present DFT + *U study in comparison to the experimental measurements* [22]. *Atomic numeration corresponds to the one shown in* Fig. 1

Bond	Calculated, Å	Experimental, Å
Ag1—N1	2.12	2.077
Ag1—N2	2.12	2.095
Ag1…Ag2	3.26	3.1418
Ag1…Ag1	3.31	3.2261
Ag2—O2	2.56	2.365
Ag2—O4	2.30	2.38
Ag2—O5	2.17	2.41
Ag2—O1	2.44	2.447
C—H	1.10	0.97

Table 2

Main angles formed by the chemical bonds in the $Ag_2(C_4H_4NO_2)_2(H_2O)$ *crystal obtained by the* DFT + *U computations in comparison to the experimental data* [22]. *Atomic numeration corresponds to the one shown in* Fig. 1

Angle	Calculated, deg.	Experimental, deg.
N1—Ag1—N2	162.0	165.55
O2—Ag2—O4	116.2	134.2
O2—Ag2—O5	91.8	79.03
O4—Ag2—O5	147.1	146.73
O2—Ag2—O1	118.9	123.74
O4—Ag2—O1	78.8	74.98
O5—Ag2—O1	76.6	87.71

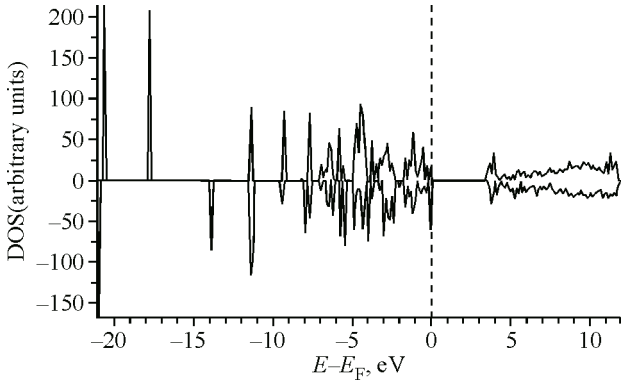

Fig. 3. Total DOS of the $Ag_2(C_4H_4NO_2)_2(H_2O)$ molecular crystal. The band-gap width is found to be approximately 3.4 eV

tisfactorily the geometry of this molecular crystal using the periodic DFT model. That implies that the periodic approach can be used for studies of at least some of the molecular crystals. It might be also stated that some discrepancy between the computational and experimental quantities could be attributed to the experimental problems in determining the correct sites for the H atoms. In the experimental measurements [22] the methylene H atoms are placed using a riding model. The computed C—H bond length (1.10 Å) is very close to the known distance between the C and H atoms in a free CH_2 complex (1.08 Å) [28]. That is why we believe the experimentally underestimated C—H distance to lead to a smaller cell volume compared to our outcome.

The spin polarised version of DFT has been used throughout the study since it was found that the system had a lower total energy if α and β electron subsystems are taken into consideration separately. The total density of states (DOS) obtained from the DFT+*U* computations reveals a pattern depicted in Fig. 3, while the partial DOS for each of the atomic orbitals (AOs) are shown in Fig. 4. There are two strong peaks around –24 eV and –22 eV for β and α spins respectively. The lower-energy peak is due to the C 2*s* and O 2*s* AOs, whereas the higher energy peak is mainly due to the O 2*s* states with a considerable admixture of C 2*s* AOs. A narrow peak around –17.5 eV in α spin is predominantly because of the N 2*s* states with a strong admixture of the C 2*s*, C 2*p* as well as O 2*s* AOs. The next narrow energy peak is observed close to –14 eV for β spin and is composed mainly of the C 2*s* AOs. The higher energy states are found to be practically symmetric for α and β spin subsystems. An energy band, which can be considered as the upper valence band (VB), extends from approximately –8 eV up to the Fermi level at 0 eV. The principal contributions to this occupied energy band come from Ag 4*d* AOs, C 2*p* AOs, N 2*p* AOs, O 2*p* AOs as well as H 1*s* states. The top of the upper VB is mainly due to the O 2*p* and Ag 4*d* AOs, so one can point to the hybridization effect between these AOs to form the edge of the upper VB.

There exists a gap of about 3.4 eV between the occupied upper VB and the unoccupied conduction band (CB) states. The lower part of CB is formed by the C 2*p* and O 2*p* states with a strong admixture of the Ag 5*s* and Ag 5*p* AOs along with some adding of the H 1*s* states. At higher energies, Ag 5*s*, Ag 5*p* as well as C 2*p* states are mainly responsible for the unoccupied energy band. A value of the band-gap width (3.4 eV) implies that the $Ag_2(C_4H_4NO_2)_2(H_2O)$ molecular crystal might be considered as a wide band-gap semiconductor. However, in order to exhibit the electrical conductivity similar to inorganic wide band-gap semiconductors, the molecular crystal should possess free electrons or free holes since typical current carriers in organic semiconductors are holes and electrons in π-bonds. Although molecular compounds are normally insulators, their constituent molecules have π-conjugated systems, and electrons can move via π-electron clouds, especially by hopping, tunnelling, or some other related mechanism.

Bader′s population analysis [29] has been exploited to calculate charges on atoms. Through the employment of this procedure it is possible to obtain a charge on a particular atom in the crystal lattice thanks to the use of a robust algorithm. The Bader population analysis shows that the O atoms have charges between –0.42 *e* and –0.96 *e* depending on their neighbours. The atoms forming chemical bonds with an Ag atom are more negative (–0.90 *e* to –0.96 *e*) compared to those O atoms of an H_2O

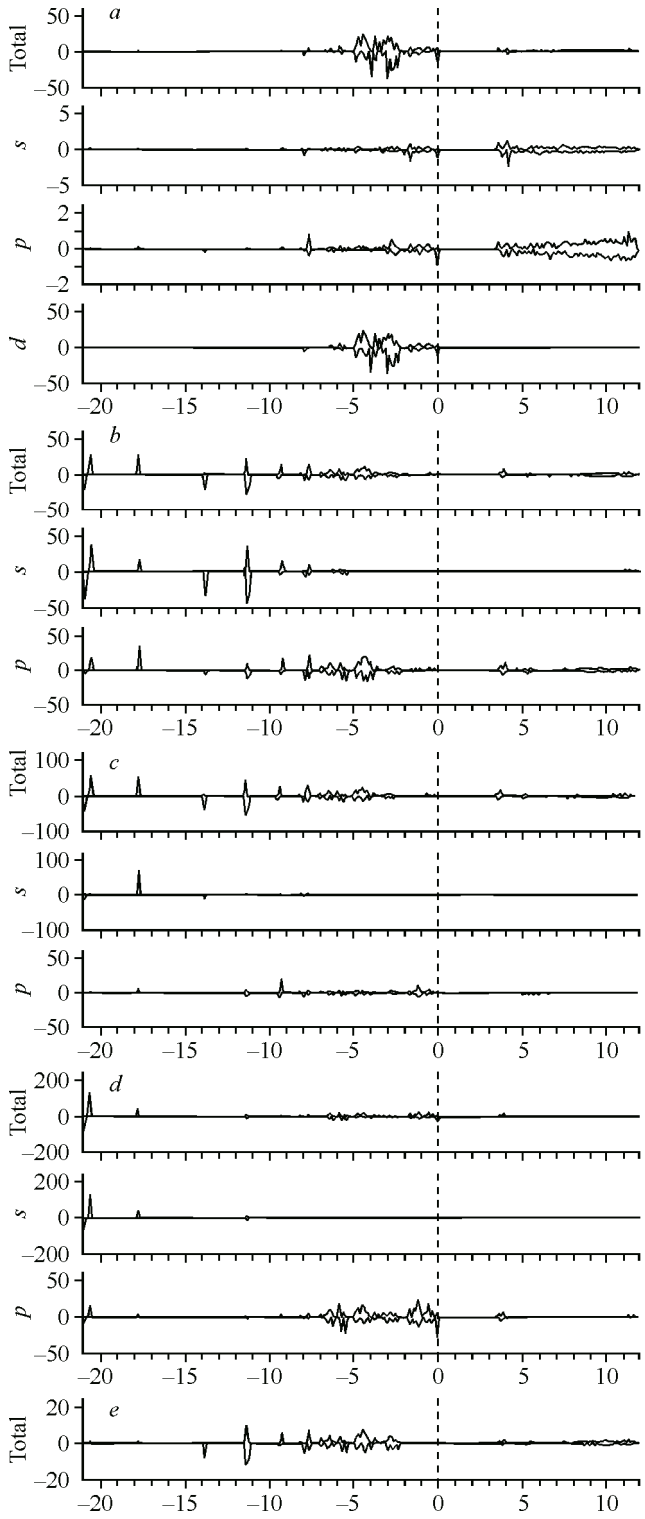

Fig. 4. Partial DOS of $Ag_2(C_4H_4NO_2)_2(H_2O)$ for the following atoms: (*a*) Ag, (*b*) C, (*c*) N, (*d*) O, and (*e*) H

complex (–0.42 *e*). The N atoms have a charge between –0.90 *e* and –0.96 *e*. There are two types of C atoms: some of them are C—N and C—O bonded, and the other are C—C and C—H bonded. For the first type of C atoms, the charges are between 0.89 *e* and 1.09 *e*, whereas the C atoms of the second type have charges between 0.01 *e* and 0.08 *e*. The Bader population analysis implies that the first type

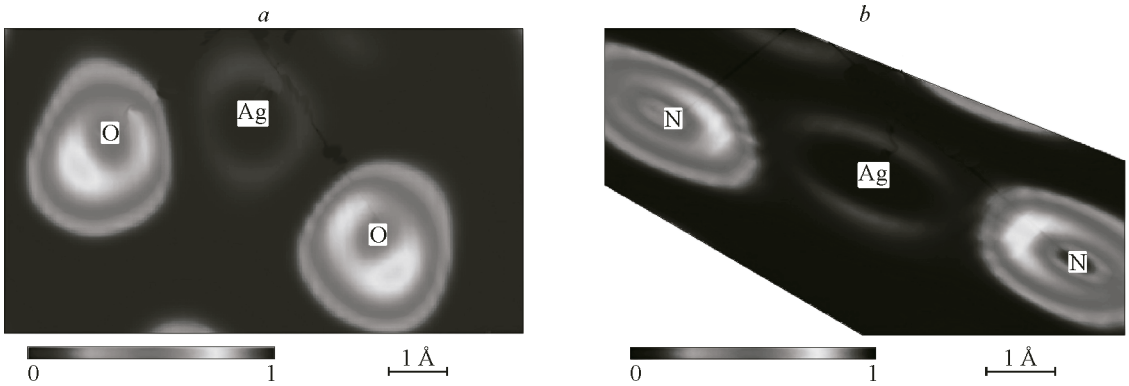

Fig. 5. Electronic density plots taken around one of the Ag atoms for (*a*) the O—Ag—O chemical bond and (*b*) the N—Ag—N chemical bond respectively.
The electronic density is mainly concentrated on the Ag-nearest O and N atoms showing the significance of the ionic character in the chemical bonding between the metal (Ag) atom and its vicinity. Nevertheless, the principal bond character can be considered as being of the coordinate covalent type

of the C atoms is more ionic compared to those forming the second type bonds which are more covalent. The H atoms have rather small charges close to 0.0 *e*. Finally, the atomic charges on the Ag atoms are between 0.42 *e* and 0.72 *e*. The obtained electron density maps for the vicinity of metal (Ag) atoms are shown in Figs. 5, *a* and 5, *b* for the O—Ag—O and N—Ag—N chemical bonds respectively. As one can notice, the metal atoms lose practically all their valence electron density. However, these electrons are not wholly transported to the Ag-nearest O and N atoms since we do not observe a considerable electron density augmentation on these atoms. The valence electrons from the Ag atoms are redistributed in the vicinity and it is implied that the Ag—O and Ag—N chemical bonds are only partially ionic with a strong covalent contribution. Actually, we can also consider this electronic arrangement as a coordinate covalent bond or a polar covalent bond since the valence electrons shared by the atoms come from the Ag atoms and the electron clouds have been shifted strongly towards the positions of the N and O atoms.

The important outcome of our investigation is the discovery of local magnetic moments on some of the O atoms situated close to the two metal (Ag) atoms. The magnitude of magnetic moments on these oxygen atoms is found to be around 1.03 μ_B. The Ag atoms also exhibit magnetic moments of 0.28 μ_B and 0.12 μ_B for the Ag atoms forming chemical bonds with the N and O atoms respectively. While the Ag atoms normally are diamagnetic [28], a free O atom is paramagnetic due to the unpaired electrons (the $2s^2 2p^4$ electron configuration) and its magnetic behaviour was well established a long time ago [30, 31]. However, due to the periodicity and consequent compensation effects O atoms/ions normally do not display any magnetic behaviour in crystals. Despite the fact that the explanation might not be definitive, we suggest that the magnetic coupling between the spins of two next-to-nearest neighbours is mediated via super-exchange or the Kramers—Anderson [32], interaction. In the $Ag_2(C_4H_4NO_2)_2(H_2O)$ molecular crystal there is a finite number of interacting spin centres, e.g. paramagnetic ions, which might lead to molecular magnetism through the super-exchange model. Outcome on the magnetic properties underlines the importance of solid-state calculations of molecular crystals since it allows the exploration of the system taking into consideration its periodicity.

CONCLUSIONS

Using the first-principles DFT+*U* electronic structure calculations the $Ag_2(C_4H_4NO_2)_2(H_2O)$ molecular crystal has been studied. We demonstrate that the periodic DFT methodology can be applied successfully to some molecular crystals since we managed to reproduce rather well the structure of this particular system. The monoclinic crystal lattice with the corresponding parameters $a = 8.74$ Å, $b = 8.09$ Å and $c = 17.82$ Å is obtained in close concordance with the available experimental data. The bond lengths and the angles between the principal chemical bonds are also found to be close to the

existing experimental results. The only disagreement is for the H bonds which are larger compared to the corresponding experimental values. Notwithstanding, this discrepancy does not necessarily mean that our results are wrong since the experimental estimation of the H positions can be erroneous.

The computed DOS of the $Ag_2(C_4H_4NO_2)_2(H_2O)$ molecular crystal implies that this crystal can be considered as a wide band-gap semiconductor with the band-gap width being close to 3.4 eV. Valence electron density plots as well as Bader charges on atoms indicate that the metal (Ag) atom has the ionic-covalent bonding with its neighbouring O and N atoms, which might be also considered as polar covalent bonds.

The obtained local magnetic moments on some of the O atoms as well as the metal atoms suggest that the particular compound might be considered for the design of future molecular magnetic materials.

The main conclusion of our paper is that the periodic DFT model can be used to reproduce rather well the crystal structure and the main geometrical parameters of at least some of the molecular crystals. This is contrary to the dominating opinion that only molecular non-periodic modeling can be used to investigate similar compounds. The availability of solid-state periodic DFT models for molecular systems allows the study of the electrical, electronic, magnetic, and other features at more precise level and thus opens new possibilities in the research of these systems at the fundamental quantum level. The cooperativity of crystallization can select and stabilize the structures that might be disfavoured or unstable in solution, hence it may be easier to make crystalline arrays of self-assembled structures than to make structures themselves. So, the process of crystallization can have a profound effect on the self-assembly at the molecular level.

Acknowledgements. Help of Marcela Cabrera at the initial stages of the computations is greatly appreciated. We also sincerely thank Richard Rivera for the assistance in managing some of the VASP files.

REFERENCES

1. *Russell A.D., Hugo W.B.* // Prog. Med. Chem. – 1994. – **31**. – P. 351.
2. *Feng Q.L., Wu J., Chen G.Q., Cui F.Z., Kim T.N., Kim J.O.* // J. Biomed. Mater. Res. – 2000. – **52**. – P. 662.
3. *Clement J.L., Jarrett P.S.* // Metal-Based Drugs. – 1994. – **1**. – P. 467.
4. *Farrell N.P.* Uses of Inorganic Chemistry Complexes in Medicine, Cambridge: RSC, 1999.
5. *Ahmad S., Isab A.A., Ali S., Al-Arfaj A.R.* // Polyhedron. – 2006. – **25**. – P. 1633.
6. *Kasuya N.C., Sato M., Amano A., Hara A., Tsuruta S., Sugie A., Nomiya K.* // Inorg. Chim. Acta. – 2008. – **361**. – P. 1267.
7. *Kasuga N.C., Yamamoto R., Hara A., Amano A., Nomiya K.* // Inorg. Chim. Acta. – 2006. – **359**. – P. 4412.
8. *Dennehy M., Tellería G.P., Tarulli S.H., Quinzani O.V., Mandolesi S.D., Guida J.A., Echeverría G.A., Piro O.E., Castellano E.E.* // Inorg. Chim. Acta. – 2007. – **360**. – P. 3169.
9. *Miyamoto T., Kitajima Y., Sugawara H., Naito T., Inabe T., Asakura K.* // J. Phys. Chem. C. – 2009. – **113**. – P. 20476.
10. *Wang D.-Z.* // J. Mol. Structure. – 2009. – **929**. – P. 128.
11. *Yang H., Lao Y.-N., Chen J.-M., Wu H.-X., Yang S.-P.* // European J. Inorg. Chem. – 2009. – **2009**. – P. 2817.
12. *Weng H.-S., Lin J.-D., Long X.-F., Li Z.-H., Lin P., Du S.-W.* // J. Solid State Chem. – 2009. – **182**. – P. 1408.
13. *Li B., Zang S.-Q., Ji C., Liang R., Hou H.-W., Wu Y.-J., Mak T.C.W.* // Dalton Trans. – 2011. – **40**. – P. 10071.
14. *Bavelaar K., Khalil R., Mutikainen I., Turpeinen U., Marques-Gallego P., Kraaijkamp M., van Albada P.G.A., Haasnoot J.G., Reedijk J.* // Inor. Chim. Acta. – 2011. – **366**. – P. 81.
15. *Kasuga N.C., Yoshikawa R., Sakai Y., Nomiya K.* // Inorg. Chem. – 2012. – **51**. – P. 1640.
16. *Koch W., Holthausen M.C.* A Chemist′s Guide to Density Functional Theory. 2nd ed., Wiley-VCH, Heidelberg, 2001.
17. *Martin R.* Electronic Structure: Basic Theory and Practical Methods, Cambridge University Press, Cambridge, 2004.
18. *Kohn W.* // Rev. Modern Phys. – 1999. – **71**. – P. 1253.
19. *Geerlings P., de Proft F., Langenaeker W.* // Chem. Rev. – 2003. – **103**. – P. 1793.
20. *Maddox J.* // Nature (London). – 1988. – **335**. – P. 201.
21. *Podeszwa R., Rice B.M., Szalewicz K.* // Phys. Rev. Lett. – 2008. – **101**. – P. 115503.

22. *Whitcomb D.R., Rajeswaran M.* // Acta Crystall. E. – 2007. – **63**. – P. m1179.
23. *Kresse G., Furthmüller J.* // Phys. Rev. B. – 1996. – **54**. – P. 11169.
24. *Perdew J.P., Chevary J.A., Vosko S.H., Jackson K.A., Pederson M.R., Singh D.J., Fiolhais C.* // Phys. Rev. B. – 1992. – **46**. – P. 6671.
25. *Kresse G., Joubert D.* // Phys. Rev. B. – 1999. – **59**. – P. 1758.
26. *Perdew J.P., Ernzerhof M., Burke K.* // Phys. Rev. Lett. – 1996. – **77**. – P. 3865.
27. *Dudarev S.L., Botton G.A., Savrasov S.Y., Humphreys C.J., Sutton A.P.* // Phys. Rev. B. – 1998. – **57**. – P. 1505.
28. *Lide D.R.* Ed., CRC Handbook of Chemistry and Physics, CRC Press, Boca Raton, 2005.
29. *Bader R.F.W.* // The International Series of Monographs on Chemistry, 22, Oxford University Press, Oxford, 1990.
30. *Kurt O.E., Phipps T.E.* // Phys. Rev. – 1929. – **34**. – P. 1357.
31. *Radford H.E., Hughes V.W.* // Phys. Rev. – 1959. – **114**. – P. 1274.
32. *Anderson P.W.* // Phys. Rev. – 1950. – **79**. – P. 350.